

SEDIMENTOLOGYthe journal of the
International Association of Sedimentologists**Controls on channel deposits of highly variable rivers:
comparing hydrology and event deposits in the Burdekin
River Australia**

Journal:	<i>Sedimentology</i>
Manuscript ID	SED-2019-OM-032
Manuscript Type:	Original Manuscript
Date Submitted by the Author:	06-Feb-2019
Complete List of Authors:	Alexander, Jan; University of East Anglia, School of Environmental Sciences Amos, Kathryn; University of Adelaide, Australian School of Petroleum Herbert, Christopher; School of Environmental Sciences Fielding, Christopher; University of Nebraska, Department of Geosciences
Keywords:	channel deposits, flood event deposits, High discharge variance river system, Antidune, unit bar

SCHOLARONE™
Manuscripts

Controls on channel deposits of highly variable rivers: comparing hydrology and event deposits in the Burdekin River Australia

Running Title: **Burdekin River hydrology and event deposits**

JAN ALEXANDER^{1*}, CHRIS HERBERT¹, CHRISTOPHER R. FIELDING² and KATHRYN J. AMOS³

¹School of Environmental Sciences, University of East Anglia, Norwich, NR4 7TJ, UK.

²Department of Geosciences, 214 Bessey Hall, University of Nebraska-Lincoln, NE 68588-0340, USA.

³Australian School of Petroleum, University of Adelaide, SA 5005, Australia.

*Corresponding author j.alexander@uea.ac.uk.

Abstract

Flood frequency, magnitude and duration all contribute to the control on river channel morphology and sedimentary architecture. In rivers with very variable discharge, illustrated herein by the Burdekin River Australia, most sediment movement is restricted to a few days each year and at other times little sediment moves. However the maximum discharge magnitude does not directly correlate with the amount of morphological change and some big events do not produce large deposit volumes. The event duration controls the work that the event can do and thus the volume of the event deposit, so that large magnitude events with short duration may cause less channel change than moderate events with longer duration. The Burdekin channel features and facies consist of five main depositional elements: a) unit bars, b) vegetation-generated bars, c) gravel sheets and lags, d)

antidune trains, and e) sand sheets. The proportions of each preserved in the deposits depend on the history of successive individual large discharge events, the duration of the events and the rate at which they wane. Floods with similar peak magnitude but different rate of decline preserve event deposits and architectures that are different. The high intra- and inter-annual discharge variability and rapid rate of stage change, make it likely that small and moderate scale bed morphology will usually be out of equilibrium. Consequently, dune and unit bar size and cross-bed set thickness are not good indicators of channel size. Antidunes may be more useful as indicators of flow depth than high-angle cross-bed sets formed by dunes or unit bars. Rivers with very high coefficient of variance of maximum discharge such as the Burdekin form distinctive channel sediment bodies, but with component parts that if examined in isolation may lead to misleading interpretation of the nature of the depositional environment if conventional interpretations are used.

Key words: High discharge variance river system, antidunes, unit bars, event deposits, channel deposits.

Introduction

Uncertainty persists as to the origins of alluvial deposits in the rock record, specifically whether they are predominantly a time-averaged amalgam of all flow events that a system experienced, or a more biased record of fewer, larger events (Sadler, 1983; Dott, 1983; Sambrook Smith *et al.*, 2010). This uncertainty is particularly acute in evaluating the alluvium of streams which exhibit extreme variations in discharge (so-called “flashy” rivers). The possibility that certain types of flow events may be disproportionately well-represented in the geological record is tacitly acknowledged in many publications, but has not been significantly quantified to date. This is because it has hitherto been challenging to create datasets entailing hydrographic records, time-sensitive, serial imagery of river beds, and synchronised ground observations of those sites. In this paper, we provide such a

dataset and use it to investigate the controls on surface deposit character and subsurface stratigraphic architecture in a river that experiences flashy discharge patterns with significant inter-annual variability, the Burdekin River of NE Australia (Fig. 1A).

In March 2017, Tropical Cyclone (TC) Debbie caused heavy rainfall over part of northern Queensland Australia, including part of the Burdekin River catchment, and resulted in a discharge event that peaked at $11\,955\text{ m}^3\text{ s}^{-1}$ at the Clare gauging station (Fig. 2A: Australian Government Bureau of Meteorology data). Research into the impact of this event on a reach of the lower Burdekin River (Fig. 1C) was undertaken with the initial rationale to consider whether large individual events such as that caused by TC Debbie would produce features in the deposit that could be diagnostic of such events in ancient deposits formed within comparable, highly variable discharge systems. The observations in 2017, combined with previous observations at the same site (Amos *et al.*, 2004; Fielding *et al.*, 2005b; Herbert *et al.*, 2018; *in press*) lead to analysis of the variation of rainfall-discharge responses in this catchment and the associated sedimentology. All of this research aims to refine the understanding of the sedimentology of variable-discharge rivers (cf. Fielding *et al.*, 2009; 2011).

In the Burdekin River, most of the sediments are deposited during large-magnitude discharge events with very little change occurring between the big discharge events. That between-event change is limited to vegetation growth, a little aeolian and biological reworking and a small volume of sediment movement in the low flow channel. Consequently, the architecture of the channel deposits results from a sequence of big events. This is unlike classic river architecture as illustrated by case studies from rivers with less variable discharge, epitomised by the Calamus River Nebraska USA (Bridge *et al.*, 1998), South Esk River Scotland (Bridge *et al.*, 1995), the South Saskatchewan (Sambrook Smith *et al.*, 2010) and the Platte River USA (Joeckel and Henebry, 2008; Horn *et al.*, 2012).

Rainfall across the Burdekin catchment occurs mainly between January and April (Australian Government Bureau of Meteorology; bom.gov.au/climate) and is mostly short-duration, intense episodes associated with tropical cyclones, smaller-scale tropical depressions and a monsoonal trough that have variable contributions across the region in successive years. In the wet season, intense rainfall may be localised or widespread and results in very large but short-duration discharge events. Droughts may last several years and frequently end in sudden heavy rainfall events.

The Burdekin River has very highly variable discharge (Fig. 2); a characteristic of many rivers in the semi-arid, seasonal tropics. This results in large variations in flow velocity, inundation depth, deposit distribution and character. Most of the time (all dry season and through most of most wet season) the discharge is low or very low and most of the channel bed is sub-aerially exposed (Fig. 1C). Droughts of multiple year duration cause prolonged low flow conditions. Widespread intense rainfall causes very rapid stage rise and high magnitude discharge events that wane quickly. The river flow stays within channel in most years, but even in those years, the intense rainfall may cause widespread flooding. Sediment movement and morphological change is restricted to a few days in each year, during and following intense rainfall, while at other times little sediment is moved.

As is common to rivers in the seasonal tropics, the Burdekin River has a very high *coefficient of annual peak discharge variation* of 1.00 (cf. Fielding *et al.*, 2018). Fielding *et al.* (2018) suggest that the sedimentary architecture of such systems is distinctly different to more steady systems. The river channels scale with the peak flow of the major flow events that may have return intervals ~10 years (Alexander *et al.*, 1999; Fielding *et al.*, 1999). This is unlike most perennial systems in other climatic settings, where “channel-forming discharge” events have return intervals of 1–2 years (Williams, 1978).

The average annual suspended sediment export of the Burdekin River to the Coral Sea has been estimated as 3.93×10^6 tonnes (80% confidence interval = $3.4\text{--}4.5 \times 10^6$ tonnes), based on 24 years of data (1986–2010; Kuhnert *et al.*, 2012). However, the annual sediment export estimates ranged from 0.004 to 15.7×10^6 tonnes (Kuhnert *et al.*, 2012), illustrating the wide variation between events. Bainbridge *et al.* (2014) found that discharge events with similar magnitudes could have substantially different suspended sediment loads. Increased suspended sediment loads have been recorded in drought-breaking floods (Mitchell & Furnas, 1996; McCulloch *et al.*, 2003; Amos *et al.*, 2004; Bainbridge *et al.*, 2014), consistent with decreasing sediment loads as vegetative ground cover increases (cf. Kuhnert *et al.*, 2012). The Burdekin Falls Dam (Fig. 1) traps all the bed load from 88% of the catchment area, but a lot of the fine silt and clay passes the dam in suspension. Most of the suspended sediment is transported through the river system to the sea and contributes only a very small proportion to the channel deposits, despite being up to 90% of the total sediment load of any discharge event. For example, in the 2000 discharge event that peaked at $11\,155 \text{ m}^3 \text{ s}^{-1}$, Amos *et al.* (2004) estimated that about 3.7×10^6 tonnes of suspended sediment and 3×10^5 tonnes of bedload were transported past the Inkerman Bridge on the coastal plain.

Fielding *et al.* (2011) observed that the distinctive characteristics of Burdekin River channel deposits and those of other lowland highly-variable discharge rivers “include: (1) *erosionally based channel-fill lithosomes that exhibit complex lateral facies changes, with (2) abundant, pedogenically modified mud partings, (3) complex internal architecture that may lack the macroform elements typical of other fluvial sediment bodies, (4) an abundance of sedimentary structures formed under high flow stage (here termed Froude-transcritical and supercritical structures: FTSS), and (5) an abundance of in situ trees that colonize channel floors and are adapted to inundation by fast flowing water*”. Fielding *et al.* (2018) suggest that the channel deposits of highly variable discharge rivers are “characterized by an abundance of sedimentary structures indicative of Froude critical and supercritical flow, preservation of abundant remains of both in situ and arborescent vegetation and transported vegetational debris (and particularly large

woody debris), pedogenically-modified mud partings within the channel deposit, abrupt lateral facies changes, and a paucity of macroform structure in the subsurface alluvial record'. They suggest that a wide range of bedding structures is preserved in a complex three-dimensional mosaic, and abundant woody material (both in situ and transported) and pedogenically modified mud layers within the channel body record multi-year droughts with low peak annual flow. Periods of multi-year droughts allow opportunistic tree species to grow on the channel bed, establishing groves that facilitate bar growth (Fielding *et al.*, 1997).

The research presented herein supplies new data to refine the understanding of the sedimentology of variable-discharge rivers (cf. Fielding *et al.*, 2009: 2011). The Burdekin River data confirm that similar rainfall events may produce flows with significantly different hazard characteristics depending on antecedent conditions (cf., Alexander *et al.*, 1999), and discharge events with similar peak magnitude may result in different event deposits depending on water and sediment routing, and the rate of change. This work establishes that the flood duration and pattern of discharge fall are important controls on the nature of the deposits and features preserved on the bed.

This paper further suggests that the concept of dominant discharge (defined as that discharge which transports most bed sediment in a stream that is close to steady-state conditions; Carling, 1988) is of no use in highly-variable discharge systems because, (a) they are unlikely to reach equilibrium with their flows (never at steady-state) and (b) the amount of work done by a flood depends not only on the peak discharge but also on the duration of exceedance of a critical discharge.

Hydrology of the Burdekin River

The large Burdekin catchment varies from semiarid continental interior to wetter coastal terrain (Fig. 3A). The topography of the catchment is mostly low, rising to 1030 m in the Star River

subcatchment within the Paluma Range in the north (Fig. 1A). The geology of the catchment is varied (Fig. 3B; Prosser *et al.*, 2002). The land use (Fig. 3C), topography and vegetation cover all affect the speed with which runoff gets into and down the river and the character and magnitude of sediment in the channel (e.g. Neil *et al.*, 2002).

In the lower Burdekin River, over the last 50 years, there have been 22 discharge events with peak magnitude greater than $10\,000\text{ m}^3\text{ s}^{-1}$ (Fig. 2, Table 1). Analysis of these, their causative rainfall and their impact on the channel bed with field observations (1998-2017), aerial photographs (1994 – 1998) and satellite images (2006-2017) lead to the categorisation of these into three event types, dependent mostly on the rate at which stage fell. (1) Events that peak in $10\,000\text{--}14\,000\text{ m}^3\text{ s}^{-1}$ range with short duration and rapid fall (that resulted from short-duration rainfall over the eastern sub-catchments) produced flashy hydrographs. These events reworked bar surfaces and produced minor bar accretion. Washed-out dunes dominated bar surfaces, and antidunes were preserved. (2) Events in the $10\,000\text{--}14\,000\text{ m}^3\text{ s}^{-1}$ range with gradual decline. These resulted from rainfall over the northern catchments, or widespread rainfall, produced hydrographs with slower falling limbs and greater total discharge volume. These events changed bar positions and produced new attached bars. Bar surfaces were dominantly sand and gravel sheets. (3) The biggest events, arbitrarily defined as greater than $14\,000\text{ m}^3\text{ s}^{-1}$. These events reworked large amounts of the bed, removed a lot of riverbed vegetation and created new bars.

The discharge in the Burdekin River and its tributaries is monitored at sites through the catchment (Australian Government Bureau of Meteorology; bom.gov.au/climate). The river has been gauged at Clare continuously since 1949. This gauge is 52 km from the river mouth (Fig. 1B) and the drainage basin area above Clare is $129\,876\text{ km}^2$. A time series of discharge recorded at Clare shows the magnitude of peak events and the variation within and between years (Fig. 2). The Burdekin Falls Dam, 160 km upstream of the river mouth, impounds Lake Dalrymple (up to 1.85 km^3 area) and was completed in 1987. The mean annual peak discharge, measured at Clare before

and since the dam was built, are $10\,430\text{ m}^3\text{ s}^{-1}$ and $6813\text{ m}^3\text{ s}^{-1}$. Since dam construction, early in the wet season, the discharge in the lower river is a little reduced as Lake Dalrymple fills, and the magnitudes of small to medium discharge events are reduced. The magnitude of large events ($> 10\,000\text{ m}^3\text{ s}^{-1}$: those considered in this paper) are little changed by the dam. The magnitude and steadiness of dry season flows appear slightly increased (about $7\text{-}30\text{ m}^3\text{ s}^{-1}$) probably because of increased local irrigation runoff.

The frequency distribution of discharge events measured at Clare suggests a natural “break” or change in the distribution pattern between $7500\text{ m}^3\text{ s}^{-1}$ and $10\,000\text{ m}^3\text{ s}^{-1}$, and another between $10\,000\text{ m}^3\text{ s}^{-1}$ and $12\,500\text{ m}^3\text{ s}^{-1}$. In addition, anecdotal evidence (see Burdekin Shire’s historic data www.burdekin.qld.gov.au/council/history-and-heritage/) suggests that when discharge reaches about $14\,000\text{ m}^3\text{ s}^{-1}$ water starts flowing from the Burdekin River into the Stokes Creek - Warren’s Gully system (a system of linear topographic lows marking palaeochannels on the right bank, across the coastal lowland to the Coral Sea; Fig. 1B). Peak discharges of $10\,000\text{ m}^3\text{ s}^{-1}$ and $14\,000\text{ m}^3\text{ s}^{-1}$ at Clare are used herein to discriminate discharge event sizes at the study site. These discriminating magnitudes are used solely for the lower Burdekin river below Clare. At other reaches of the river system similar discharge classes can be defined (as below) but as channel size differs, so does defining discharge. Individual runoff events may behave differently in different parts of the river. For example, attenuation of flood waves down the river system result in some large magnitude events in mid reach being moderate peak events in the lower river. For example, in 1997, discharge measured at Sellheim peaked over $16\,000\text{ m}^3\text{ s}^{-1}$ and declined quickly, but there was little rain in other parts of the catchment and the flood wave peaked at $7228\text{ m}^3\text{ s}^{-1}$ at Clare (Fig. 2B). Observations above Charters Towers at Big Bend and Dalrymple (Fielding *et al.*, 1999; Fig.1A) suggest that this event reworked entire bars at that site but may have had little impact downstream at the study site near the Inkerman Bridge.

The Lower Burdekin River Study Reach

The study reach (Fig. 1) is at the downstream end of a nearly straight, 10 km-long section of the Burdekin River. The reach extends 10 km from Inkerman Bridge (19°38'8.58"S 147°24'14.40"E) to the difffluence of the main channel and Anabranh (first distributary; Fig. 1B). The channel bed is easily accessible and has been studied at intervals since 1998 (e.g., Amos *et al.*, 2004; Fielding *et al.*, 2005a, 2005b; Alexander & Fielding, 2006, Herbert & Alexander, 2018). Multiple aerial photographs (1994 – 1998) and satellite images (2006-2017) have been analysed. It has been possible to assess the changes in the bed morphology before and after some individual events. Fieldwork has included topographic surveying, observation of river and floodplain sediments, vegetation surveys, trenching, coring, sediment sampling (subsequent granulometry and compositional analysis), ground-penetrating radar surveys, observations and sampling of discharge events, and acquisition of rainfall and discharge data from other sources.

The channel width within the study reach varies from 700 to 1900 m (mean 1187 m). The bank top height varies along each bank and bed-sediment mobilisation during discharge events causes changes in channel depth in space and time. Consequently the “*bank-full depth*” is not easy to define, but is around 10 m. The main banks of the channel are generally steep and vegetated. The channel floor by comparison is generally low gradient, sloping across or down the channel or composed of multiple ridges (Fig. 4). During the dry season, most of the riverbed is emergent and easy to observe, but the very deepest parts of the channel could not be observed directly or measured, because they are water-filled even in dry conditions. These lows can be seen in the photograph in Fig. 5 and represent a small proportion of the channel bed area. This pattern gives the low stage river the appearance of “*pool and riffle*”, but the morphology is created by bar formation and bar movement during large discharge events. The pattern does not change much, if at all at low stage (most of the year).

Riparian vegetation is important in the Burdekin River. The prolonged exposure of large areas of river bed allows vegetation growth, which subsequently influences sedimentary processes (Fielding *et al.*, 1997; Nakayama *et al.*, 2002). During wet periods, seeds germinate rapidly, and in the tropical climate plants grow rapidly if they can access water (which they can if their roots can reach the water table in the channel deposits). Through multi-year droughts, the vegetation can grow to considerable size and this influences the subsequent bar development. Very large discharge events strip most, or all, of the vegetation from the channel bed, or bury it.

The catchment is large and the geology is varied (Fig. 3B). This generates sediment with varied composition, which can be transported rapidly down the system. The water impounded by the Burdekin Falls Dam traps a lot of the sediment from the upper catchment and most of the coarse component of the load (Lewis *et al.*, 2013). Over a 5-year monitoring period (2005/2006 to 2009/2010), Lewis *et al.* (2013) measured the trapping efficiency of the reservoir at between 50% and 85%. They found that particles $<0.5 \mu\text{m}$ passed over the dam spillway; 50% of particles $0.5\text{--}5.0 \mu\text{m}$ were trapped in the reservoir; 75% of particles $5.0\text{--}30 \mu\text{m}$ were trapped and 95% of particles $>30 \mu\text{m}$ were trapped. Consequently, since completion of the dam, in addition to reworking existing bed and bank sediment, additional coarse sediment entering the lower river is derived from the Bowen-Bogie catchments and local runoff into the channel, whereas fine sediment comes from any part of the catchment.

During most of the year, much of the channel sediment is dry and composed of moderately sorted coarse sand and gravelly sand that is compositionally immature, with pebbles and cobbles of a wide range of lithologies. Sand from different parts of the catchment is not easily recognised, although that from the southern sub-catchments can be distinguished by the magnetic properties of magnetic inclusions within silicate grains (Maher *et al.*, 2009). Since 1987 it is likely that little sand has moved past the Burdekin Falls Dam, but coarse sediment derived from the catchment above the dam before then is still moving down the lower river. Based on magnetic fingerprinting, sand

fractions of suspended sediment samples from the 2000 Burdekin flood, collected from the Inkerman Bridge, appear to have had a different source compared with those from floods in 1998 and 1999 (Maher *et al.*, 2009).

The river sediment load ranges from clay-grade wash load to sand and gravel bed load (Amos *et al.*, 2004). The clay grade sediment, although accounting for large amount of the river's transported load (e.g. Bainbridge *et al.*, 2014; 2016), is not deposited within the channel in any significant volume. Mud accounts for a very small percent of the channel bed deposits seen in trenches. In some years, mud drapes have been observed on parts of the bed, and these are also recorded in some trenches (Herbert *et al.*, *submitted*). The mud drapes are rarely more than a 1-2 cm thick, and they desiccate, break into flakes, and produce mud clasts. Mud also sometimes infiltrates the top of the sand and gravel bed. Sand is also carried in suspension in moderate and big events (Amos *et al.*, 2004; Lewis *et al.*, 2013), and a relatively high proportion of the floodplain deposits are sandy (Alexander & Fielding, 2006).

Large peak-magnitude floods and rainfall patterns

Rain mostly falls between December and April in the Burdekin catchment. Individual rain events are usually short and intense. The runoff response to rainfall depends not only on the precipitation intensity, but also on the rain duration, aerial extent, soil infiltration capacity and antecedent conditions. Intense rainfall associated with tropical cyclones and storms has been recorded within the Burdekin catchment exceeding 390 mm on 1st March 1988 at Home Hill (19.67° S 147.42° E) and 470 mm on 6th Feb 1947 at Kalamia Estate (19.52° S 147.42° E; Australian Bureau of Meteorology: www.bom.gov.au/climate/data/index.shtml). Rainfall recorded at Majors Creek (19.60° S 146.93° E), in an adjacent catchment, exceeded 510 mm on 11th January 1998, and 760 mm on 3rd March 1946. Given the spatially erratic distribution of rain gauges over the area, and availability of reliable historic data, it is likely that intensities as high or higher than these have occurred elsewhere within the catchment. Compared to tropical cyclones, a monsoon trough over

the catchment (as in 2000) produces more widespread but generally less intense rainfall, that may occur over a longer period (multiple days).

There is no widely agreed definition of *intense rain* as the use of the term depends on the experience of the individual, varying with climatic setting. It might be best related to local event frequency thresholds (cf. Groisman *et al.*, 2005). Defining what is an intense rainfall event depends on the local conditions and on the timing resolution of rainfall data. In the more humid coastal areas of the Burdekin catchment, rainfall events with over 100 mm/day are called intense rainfall events. Inland in more generally arid areas of the catchment, 50 mm/day or less rain may have a big effect on soil erosion and river response, and can be called an intense rainfall event. Part of the reason for this is that very high intensity rain over short periods (minutes), which exceeds infiltration capacity, generates rapid runoff. The use herein of *intense rainfall* for these events is comparable with the use of "intense rainfall" for short duration events of 20 mm per hour in the Caribbean (Barclay *et al.*, 2007). The pattern of rain over the catchment that triggers big discharge events is variable as is illustrated by the catchment maps of rain recorded in the 7 days pre-event and post peak discharge (Fig. 6).

During or soon after a period of intense rain, the stream stage rises extremely rapidly and in most discharge events stage also declines rapidly (Fig 7). The hydrographs measured at Clare, and other sites in the lower reaches of the Burdekin, record flood peaks moving down the system from different parts of the catchment such that the catchment network pattern in addition to the rainfall intensity and distribution, influence the character of the discharge events at the study reach. The consequence of this is that similar rainfall volume/duration events may generate different discharge hydrographs depending on the part of the catchment on which it rained, in addition to differences in rainfall events generating different patterns. Despite the large number of controls on the character and peak magnitude of discharge events, some size-duration patterns appear to be inherent in the system.

On the basis of magnitude and duration, the large peak-magnitude floods in the lower Burdekin River can be divided into three Types:

1. Events that peak in 10 000-14 000 m³ s⁻¹ range with short duration and rapid fall;
2. Events in 10 000-14 000 m³ s⁻¹ range with gradual decline and a large total discharge volume; and
3. The biggest events (>14 000 m³ s⁻¹).

The distinction between Types 1 and 2 is seen in the rate of decline of the flood and the flood duration (Fig. 7B).

The Australian Bureau of Meteorology define low flow level at Inkerman Bridge at 3 m, minor flood level as 7 m, moderate flood as 10 m and major flood depth as 12 m. For example, the level in March 2017 was classed as moderate flow on this basis, and all the other events described as large peak-magnitude floods in this paper exceeded the moderate level.

1. Events that peak in 10 000-14 000 m³ s⁻¹ range with short duration and rapid fall

In two of the events recorded at Clare that peaked in the range 10 000-14 000 m³ s⁻¹, the water level receded very quickly. These occurred in 2017 and 1988, when there was a short period of very intense rainfall on the eastern part of the catchment (Bowen-Bogie sub catchments; Fig 6). The same pattern of rapid rise and fall has also been observed in other parts of the Burdekin catchment in different years, notably recorded at Sellheim in 1997 (Fig. 2) when rain fell on the upper Burdekin catchment but not elsewhere.

The 2017 discharge event (Fig. 6) was the result of rain associated with TC Debbie. TC Debbie made landfall as a Category 4 cyclone near Airlie Beach, Queensland, Australia on 28th March 2017 (Fig. 3D) and moved inland depositing vast amounts of rain over the southeast part of the Burdekin catchment and other catchments to the south (Fig. 6). This was the first cyclone to hit Queensland in two years and followed five years of very low flow in the Burdekin River (Fig. 2).

The sudden intense rain (e.g. 36 mm/hr at 15:00 on 29th March at Urannah 20.92 S 148.32 E; Queensland Department of Natural Resources, Mines and Energy) caused very rapid runoff. Within the Burdekin catchment, rain fell mostly on the Bowen and Bogie subcatchments, which drain into the Burdekin River below the Burdekin Falls Dam. Discharge data from the Burdekin River above the Bowen River confluence demonstrates that the western and northern parts of the catchment contributed little to the flood event. At Inkerman Bridge, water level increased 6 m in 6 hours on 29th March.

The intense rain and runoff caused land degradation, entrained large volumes of sediment, changed river bed morphology and discharged a plume of fresh water and suspended sediment into the Coral Sea. The sediment flux appears to have been particularly high (preliminary data suggests total load of c.1.5 million tonnes over 6 days: Stephen Lewis *pers. comm.*). This is probably because the intense rainfall followed a prolonged dry period. This is likely similar to the pattern recorded in other drought-breaking rainfall events (Mitchell & Furnas, 1996; McCulloch *et al.*, 2003; Amos *et al.*, 2004; Bainbridge *et al.*, 2014).

2. Events in 10 000-14 000 m³ s⁻¹ range with gradual decline

In the last 50 years, there have been 12 large discharge events in which the peak was in the range 10 000-14 000 m³ s⁻¹, and in 10 of these the water level receded over a week or more. In some cases, as illustrated by 2000, 1998 and 1983, rain fell on north and central parts of catchment. In others, illustrated by 2010-11 and 2007, rainfall was more widespread (Fig. 6). In addition to those 10 large discrete events, there was another of similar character that occurred as a sub-peak of larger events in 1991. In this 1991 event, widespread rain caused discharge to rise gradually to a peak of 12 632 m³ s⁻¹ on 15th January and discharge then fell gradually.

The 2000 discharge event peaked at 11 155 m³s⁻¹ and the hydrograph recorded at Clare shows the very rapid rise and less steep falling limb (Fig. 7). In 2000, rain near the coast in January

and February produced small flows in the river at the study site. TC Steve took a track north of the catchment (Fig. 3D) and some associated rain fell on the northern parts. This was followed by rain associated with the monsoon trough along the coast and inland over the north of the catchment.

The sediment transport behaviour in the lower Burdekin River in 2000 was sediment-limited; the river could have transported more if more had been available (Amos *et al.*, 2004). The water emanated from the catchment above the Burdekin Falls Dam and followed a moderately wet year.

3. The biggest events (peak over 14 000 m³ s⁻¹)

In the last 50 years, 10 floods have peaked over 14 000 m³ s⁻¹ at Clare. Three of these peaks occurred in 1991 (Fig. 7), two in 2008 and two in 2009. Big events also occurred in 1978, 1989 and 2012 (Table 1, Fig. 2A).

For illustration, in 1991 the catchment was already wet at the start of the year and rain caused the discharge at Clare to rise rapidly to a peak of 15 709 m³ s⁻¹ on 4th January (Fig. 7), after which it fell rapidly before more widespread rain caused it to rise gradually to a peak of 12 632 m³ s⁻¹ on 15th January. The discharge fell gradually. On February 2nd 1991 rain associated with a tropical low fell over the Bowen-Broken River subcatchment, producing a discharge peak of 29 824 m³ s⁻¹ at Clare on February 3rd. This event had little contribution from the areas of catchment above the Burdekin Falls Dam, and the water level rose and fell very quickly. Discharge rose again to 12 269 m³ s⁻¹ on 9th February, and again to 20 002 m³ s⁻¹ on the 21st. Thus, not only were there three individual very big peak magnitude events, there were also two big events that would individually fit into the two categories above. Discharge was high throughout the first three months of the year.

The consequence of this was widespread reworking of most bars in the channel (cf. Fielding *et al.*, 1999). Thus 1991 effectively “re-set” the channel architecture. In addition, the duration of high flow would have allowed large bedforms to grow and give more time for large scale cross-

stratification to form, consistent with the observations from GPR data presented by Fielding *et al.*, 1999, 2011).

The 2008/2009 wet season differed from that in 1991 in that most of the discharge in the river was from the upper Burdekin subcatchment. It was a double-peaked event reaching a maximum of $19\,514\text{ m}^3\text{ s}^{-1}$ on 6th Feb 2009 and $15\,845\text{ m}^3\text{ s}^{-1}$ on 24th Feb. The discharge measured at Clare stayed above $9\,500\text{ m}^3\text{ s}^{-1}$ for 15 days. Anecdotal evidence, and comparison of satellite images from the year before and after, suggest major changes in the pattern of the river bed through this event, but we do not have adequate data to document it.

Sediment features and resulting facies associations

The channel bed examined on emergent surfaces and trenches at the study reach is dominantly coarse to very coarse sand and gravel. Sediment sampling during discharge events (e.g. Amos *et al.*, 2004; Bainbridge *et al.*, 2012; 2016; 2018) indicates transport of vast quantities of clay, silt and fine sand, but little of this is deposited in the reach. Sand and gravel is transported on the bed and in near bed suspension in big events (Amos *et al.*, 2004). This is observed on the bed and lodged in riparian trees above the bed (Fig. 8).

The channel bed is characterised by seven components: (A) sand sheets (dune fields, washed out dune fields and upper stage plane beds, (B) mud sheets, (C) gravel sheets, (D) antidune trains, (E) unit bars, (F) vegetation-obstacle marks or “fields” of such obstacle marks, and (G) vegetation-generated bars, each of which form characteristic sedimentary packages. These can combine into complex bars, or channel aggradation packages.

A. Sand sheets

Extensive sand sheets occur both as stoss-side components of unit bars and adjacent to unit bars at all elevations in the channel. When observed on the emergent bed in dry seasons, their upper

surface may be upper phase plane beds, dunes or washed out dunes (Fig. 8B). The sheets range in thickness from a few millimetres to tens of centimetres, and lateral extent from tens to hundreds of metres. The internal character ranges from planar lamination to cross-stratification. The sheet shapes vary, tending to be wedge shaped when formed on the stoss-side of unit bars and more lens shaped in other sites.

B. Mud drapes

Mud drapes are commonly observed on the emergent bed, sometimes restricted to local topographic lows, and are seen in locally in trenches (Fig. 8C). They vary in thickness from millimetres to several centimetres. Invariably they become desiccated soon after deposition. Where the drapes are millimetres thick and resting on coarse sand, desiccation can lead to mud curl formation (Fig. 8D) and these mud curls are easily reworked by small runoff events.

Mud sheets form during the waning phase of any size flood, so they are not indicative of low flow conditions. They occur at all levels in the channel and are preserved at all levels in the deposit, both as layers and as mud chips. Mud drapes tend to form when water level is relatively static or falls slowly over a few days following a bigger event. This appears more common in intermediate stages; mud drapes have been observed at low and intermediate heights on the emergent river bed. Although occasionally they are extensive over areas tens to hundreds of metres long, they are generally discontinuous, occurring particularly in areas where flow is slowed such that silt may settle from suspension. On high areas of the river bed this generally only occurs in areas where water is temporarily pooled (e.g. in the troughs between unit bars, or in scour hollows near river-bed trees).

The amount of the mud in the channel deposits and in the floodplain deposits (Alexander & Fielding, 2006) is not indicative of the proportion of the sediment load that is mud (Lewis *et al.*, 2013; Bainbridge *et al.*, 2016) as most of this is washed through the river.

C. Gravel sheets and lags

Gravel moves over the bed as isolated clasts, rolling, saltating and sometimes in modified suspension (Amos *et al.*, 2004). It moves both as isolated clasts and probably also as “carpets” over the bed. Gravel sheets have lateral extents varying from a few metres to hundreds of metres. Their thickness is rarely more than one pebble or cobble thick but can be thicker in more laterally extensive sheets. Gravel streaks are occasionally observed on flat portions of the channel bed illustrating the path of pebbles and cobbles over the surface. Gravel lags are observed in the lee of bars and obstacles and also in scours (e.g. horse-shoe shaped scours formed upstream of river-bed trees) where the gravel bed shape and extent are controlled by the scour (Fig 8F). In places, gravel sheets were partially split into structures inferred to be of antidune origin, and at some sites trains of antidunes were fully formed, suggesting that there is a spectrum observed from irregular gravel sheets to preserved antidune trains.

In the study reach the gravel is dominantly pebble or cobble grade. When observed in trenches the gravel sheets and lags generally have sand matrix, which may have been deposited with the gravel or infiltrated subsequently. The fabric (e.g. visible in the photographs in Fig. 8E) varies, but is generally imbricated either long-axis transverse or locally long-axis parallel to interpreted flow direction.

D. Antidune trains

Antidunes have been observed on the bed of the Burdekin River at several different sites and after discharge events of differing magnitudes. At the 2017 study site, antidunes were observed in two locations (‘Inkerman’ and ‘Jarvisfield’; Fig. 1C). Antidunes were observed in trains of up to six, with near parallel crestlines transverse to high-flow direction. The plan-view crest shapes varied from near straight to linguoid. At the Inkerman antidune locality, the mean wavelengths within antidune trains were between 16.4 and 28.8 m and the amplitude measured on the emergent dry bed was 0.2 to 0.5 m. Further downstream at the Jarvis field site, the wavelengths were as much as 30.7 m. All of these antidunes had steeper stoss than lee sides (3-14° and 1-6°, respectively). The

antidunes were particularly recognisable where they had an elongate gravel patch along their crests (Fig. 9A). Antidunes may have been overlooked where there was no gravel patch as the topographic expression is low. Within the Inkerman antidune field, the gravel patches at antidune crests varied up to one third of the mean antidune wavelength. When examined in section, the gravel deposits consist of a lens of sandy gravel (Fig. 9B). In a trench through one of these, the internal character was of downstream dipping cross-stratification.

The 2017 antidunes were very similar in morphology and grain-size to antidunes described at mid-catchment Burdekin River sites by Alexander and Fielding (1997). They observed trains of 3-12 parallel-crested bedforms with straight to slightly sinuous crests, wavelength from 8 to 19 m, and preserved amplitudes up to 1 m. In the antidunes described by Alexander and Fielding (1997) the gravel lenses contained single low-angle downstream-dipping cross beds, picked out by gravel stringers. The fabric within the gravel was steeply dipping.

Trains of antidunes are recognizable on satellite images and aerial photographs and recorded on the ground in some years such as 2017, while in other years, such as in 1998 (reported by Fielding *et al.*, 2005b) no antidunes were observed.

E. Unit bars and bar deposits

Relatively unmodified bars with morphologies that have developed mostly from depositional processes are termed unit bars (cf. Smith, 1974). In the Burdekin River, unit bars (Fig. 9C) are a common feature found across all but the highest elevations of the exposed river bed (Herbert *et al.*, *submitted*). They may form and move in individual discharge events and may persist for several small to moderate sized events.

Unit bars examined in the 2015 – 2017 field campaigns were hundreds of metres long and wide, and up to 0.5 m high. Their profile consisted of a very shallow dipping, planar stoss side that changed down-palaeoflow into a high-angle avalanche face. Some bars had superimposed dunes on their stoss, which were often preserved on the dry river bed in partially washed out forms

(presumably modified during falling stage). Well-preserved superimposed dunes were more common in 2017, and these were up to 0.1 m high and 0.9 m long. Dunes also commonly flanked the margins of unit bars in 2017.

Trenches through unit bars in 2017 (e.g. Fig 9D) showed the internal structure was dominated by co-sets of down-climbing cross-stratification (< 0.4 m thick). Individual sets tended to thicken as they down-climbed. In most bars, there was a transition down-flow from down-climbing cross-stratified facies into a single, relatively thick (< 0.5 m) but short (< 1 m long), planar cross-stratified deposit close to their avalanche face. Overlying these deposits were topsets of thin (< 50 mm), planar-stratified and low-angle cross-stratified sets with multiple internal truncation surfaces. Thin, localised bottomsets (< 100 mm) of gravelly mud were observed infrequently (cf. Herbert & Alexander, 2018).

Ground penetrating radar data collected in 1999 (see Fig. 6. in Fielding *et al.*, 2011) show cross-stratification on the scale of 2-5 m sets in the lower part of the channel fill. In places there is evidence of smaller sets migrating over the bigger sets. We have no direct way to establish how these formed, but it is likely that they record advancing bar fronts. Fielding *et al.* (2005b) reported that “*During the 1998, 1999, and 2000 dry seasons (May to October), large parts of the exposed riverbed surface were plane beds associated with isolated slipfaces or surfaces sloping gently towards the low-stage channel. Small parts of the surface, particularly near the low-stage channel, were gravel-armored. Elsewhere, bar surfaces were covered by fields of sinuous-crested dunes (amplitude up to 0.8 m), or locally larger, flat-topped, linguoid bedforms*” [unit bars]. The preceding wet season included a flow of 11 905 m³ s⁻¹ in January 1998, but 1992-1997 were dry years. Therefore, it is likely that these large bar sets formed in the very large discharges of 1991 (see below).

F. Vegetation obstacle marks – scours and sediment tails

Obstacle marks (Fig. 9E) result from deformation of flow by obstacles in a current (Dzulynski & Walton, 1965). Vegetation obstacle marks (cf. Nakayama *et al.*, 2002) consist of a scour around the plant(s) and a tail of sediment deposited in the lee-side separation eddy. The amounts, types and sizes of plants occurring in the channel at any one time are controlled by the interval since inundation, the species germination and growth rates, as illustrated by photographs before and after the 2017 discharge event (Fig. 5). Herbaceous vegetation germinates and grows rapidly but because of the aridity and coarse sediment of the channel floor, does not persist if there is a multiple-year drought. In contrast, some species germinate and grow rapidly and are either drought-resistant or have long roots. Most channel floor vegetation is removed, irrecoverably damaged (by breakage, abrasion or immersion) or buried by the successive event, but some species are adapted to persist successive immersion.

G. Vegetation-generated bars and channel bed in situ trees

Where areas of the bed are emergent for several years, dense groves of saplings become established. The principal types are species of *Melaleuca* and *Acacia*. In the lower river, as illustrated herein from the study site downstream of Inkerman Bridge, there are very few individual trees observed that were evidently more than about 10 years old, and most appeared less than 5 years (judging from trunk size, cf. Fielding *et al.*, 1997). This contrasts with the more common occurrence of older trees in the river bed at a study site mid catchment study site near Charters Towers (Fielding *et al.*, 1997). The reasons for this may be more frequent major inundation and also thicker channel bed deposits; at the upper river site tree roots may grow down below the basal erosion surface so that they are less likely to be uprooted. Fielding *et al.* (1997) and Fielding & Alexander (1996) demonstrated that saplings of the paperbark tree *Melaleuca argentea* that grow quickly in the channel influence sediment transport and bar formation (Fig 9F). The bars are elongate parallel to the tree groves, that may be aligned with or near to the channel direction. They are ridges of sand

and gravel that extend through the groove and in a tail on its lee side. Internal structure of such bars includes common internal erosion surfaces and sets of cross-bedding aligned in multiple directions, with single clast gravel layers lining erosion surfaces.

In the lower Burdekin River, the five years prior to the TC Debbie flow of March 2017 were a period of low discharge (Fig. 2). During this time, aerial imagery shows that significant portions of lower bar surfaces became vegetated by opportunistic plant types. Among these, *Melaleuca argentea* was the most common, but two *Acacia* species also grew in sizeable groves, and other opportunists, including shrub-like woody weeds, were locally represented. Dendrochronological examination of tree cross-sections in July 2017 indicated that all of them were less than five years old. Our site surveys carried out in July 2017 indicated that large parts of formerly closely-spaced groves on the lower bar had been entirely or substantially excised, and equally large areas were covered in dead trees, while other areas were substantially undamaged. Of the different opportunistic vegetation types, *Melaleuca* was evidently best adapted to survival owing to its specialised strategies (Fielding *et al.*, 1997) that include inclined to prostrate stance, upstream-trailing roots in the subsurface, thick, spongy bark, and subaerial root networks. Other tree types, notably *Acacia longifolia*, were of a more upright stance, and many were toppled by the flow and had suffered exhumation of their root mass. Many dead *Acacia* had been toppled by rotation of the entire tree, and were partially or completely uprooted or exhumed from their substrate. Other upright trees and saplings had been snapped at heights of 1-2 m from the bed. The greatest variability in bar topography was found among groves of mostly dead *Acacia* trees, whereas linear groves of mostly live *Melaleuca* showed subdued topography.

Depositional Models for the three different styles of discharge event

Although all the big events in this river system produce all six of the sediment packages described above, the proportions of them differ as do their position and detailed characteristics among the three flow event types.

1. Events that peak in 10 000-14 000 m³ s⁻¹ range with short duration and rapid fall

In comparison with fluvial deposits in other climatic settings, more high-stage features are preserved in all runoff events because of the rapid waning. However, in these events with rapid onset and very rapid falling stage, such features are even better preserved. After Type 1 events the river bed will preserve areas of gravelly antidunes, “washed-out” dunes, dunes, and plane bed with primary current lineation. In addition, small dunes, rills, and small obstacle marks with directions at a high angle to the mean channel direction may record rapid flow draining off the higher parts of the bed. Locally, these runoff features may be oriented up-channel recording water flowing off the up-channel side of bars into lows. These may preserve palaeocurrent patterns that are more varied than expected in fluvial systems and may appear similar to some features seen in tidal settings. There is little reworking of pre-existing unit bars.

2. Events in 10 000-14 000 m³ s⁻¹ range with gradual decline and large total discharge volume

In events with more gradual decline in discharge, preservation of high stage features is less common. This is because the flow velocity may decline during waning stage such that stationary waves are less frequent and antidunes either do not form or are not preserved because of sediment movement on the bed at later stages of flow. For example, no antidunes are recognized on aerial photographs from some years (e.g., 1998, following the event that peaked at 11 905 m³ s⁻¹ with moderately gradual decline). The dunes may be washed out as the water level declines and the bed is mostly characterised by planar beds of extensive sand sheets, gravel sheets and unit bars. The unit bars may have pre-existed but are likely to have been greatly reworked, and some are washed out.

3. The biggest events (>14 000 m³ s⁻¹)

These events rework large areas of the channel bed and produce new large bedforms and bar forms. Unit bars formed in antecedent events are likely to be removed and new ones formed. The GPR data (Fielding *et al.*, 1999, 2011) suggest that cross sets to 5 m thick are preserved deep in the channel deposits. Vegetation obstacle marks and vegetation-generated bars are likely to be less common in the deposits of these large events because of both the magnitude of the event and the duration of inundation, that will remove a lot of the river-bed vegetation, kill others by the prolonged submergence and bury still more *in situ* by complex bar formation (Fielding *et al.*, 1997).

Discussion

The ability of a discharge event to change the morphology of a river bed and banks is controlled by the rate of coarse sediment entrainment and bed load transport, as well as deposition. The volume of suspended sediment passing through the channel is of little importance in this setting as very little of it is deposited within the channel or on the banks. Volume of river-bed sediment reworked and features in sediment may not relate to the peak magnitude (magnitude or timing) of an event. The pulses of sediment input and pulses of sediment movement at any one point on the bed may not be in phase with water runoff at a site. This is seen in the data from the March 2000 discharge event (Amos *et al.*, 2004), when bedload transport rate and the rate of change in channel shape at the study site were greatest several days after the peak discharge.

Amos *et al.* (2004) estimated 3×10^5 tonnes of bedload were transported past the Inkerman Bridge in the 2000 discharge event that peaked on 25 February at $11\,155 \text{ m}^3 \text{ s}^{-1}$. They measured the average bedload transport rate (channel width-integrated) rising rapidly to $0.816 \text{ kg s}^{-1} \text{ m}^{-1}$ on 3 March and then decreasing rapidly to $0.058 \text{ kg s}^{-1} \text{ m}^{-1}$ on 6 March, then more slowly to $0.003 \text{ kg s}^{-1} \text{ m}^{-1}$ on 8th March at the end of the sampling period. If the solid sediment is considered to have a density of quartz (2648 kg/m^3) and the deposits in a newly formed unit bar a porosity of 40% then on 3 March 2000 a one metre high bar slip face could have advanced 1 m in 32.5 minutes. Whereas

on 6th March 2000 it would have taken 7.6 hours and on 8th March more than 6 days. The pulses of bedload movement will alter channel morphology by promoting bar migration and as the bedload flux lags discharge change, most bar modification occurs after peak discharge. This explains why bars are not modified much in short duration large events.

Because of the highly variable system, the Burdekin River channel is unlikely to reach a steady-state in any individual discharge event. The amount of work done by a flood depends not only on the peak discharge but also on the duration of exceedance of critical discharges. It takes time to erode bed and banks, such that the channel size and shape may not change much due to erosion in a short duration event. There is also the issue of lag time for bed accretion, because not only does it take time to entrain sediment, it also takes time for sediment to move into and down the river. This is particularly well illustrated by the 2000 event where peak bedload flux lagged peak discharge, and change would be supply-limited. Thus, the concept of dominant discharge (defined as that discharge which transports most bed sediment in a stream that is close to steady-state conditions; Carling, 1988) is of little use in these settings with very high discharge variability.

Sediment grade is not a good indicator of palaeoflow conditions in these systems. Sediment entrainment and transport is dependent on the bed shear stress, and grade of sediment in deposits is often used as a rough indication of flow depth and velocity. This is complicated in rapidly varying systems such as the Burdekin, because in rapidly changing floods the impulse force due to rapid change must also be considered (Alexander & Cooker, 2016). The velocities recorded in some Burdekin events (e.g. Amos *et al.*, 2004) and estimated from antidune morphology (e.g. for the 2017 event herein) would produce bed shear stress that could easily move particles coarser than are commonly seen on the bed. Locally where large clasts are available (road bridge debris) they are moved by big events. For example, a 1m length of steel guard rail moved about 50 m downstream from a road bridge on the Bowen tributary in the 2017 event.

The grade of sediment preserved in a deposit, however, depends not on the transport and entrainment controls but on the depositional conditions, and in a rapidly waning flood these may be significantly different to the peak conditions. The grade also depends on sediment availability and the lag time for coarse sediment to be transported to the site of deposition. At the study site, velocities and bed conditions must be such in big floods as to be capable of transporting boulder grade particles, but these are rarely available to the site. Grade therefore is a very poor indicator of peak flow conditions even in relatively small floods.

Cross-bed set thickness is not a good indicator of palaeoflow conditions in these systems.

Cross-bed set thickness has been used as an indicator of flow depth and conditions in interpreting some rock record examples (Leclair & Bridge, 2001), although Bradley and Venditti (2017) argue that there is more variability in the ratio between set thickness and flow depth and more complexity in the controls on dune scale than considered by Leclair and Bridge (2001). In the Burdekin River and similar highly variable discharge rivers, dune height and cross set thickness may be very misleading. This is both because of the speed of change and because of the occurrence of unit bars and dunes together. As dunes tend to downclimb unit bars, it leads to greater dune-set preservation than would be expected from relationships developed in the laboratory (e.g. Leclair & Bridge, 2001). Amos *et al.* (2004) pointed out that “the lag time for dune formation (particularly bigger forms) is such that there is not a strong correlation between discharge stage and dune size” in this system where stage can change by several metres in a day or two. As stage rises, dune height and length will tend to increase, but as stage rise is very fast the dune height is likely to continue to rise at and after the peak. In very flashy events the very rapid stage fall may prevent dunes ever reaching a size consistent with the magnitude of the peak. In contrast, in the very large floods with longer durations, dunes may grow bigger. In general, unit bars are larger in volume than dunes, and take longer to change length and height at the same bed load flux. Unit bar height is controlled by the “profile of equilibrium” (cf. Jopling, 1966), where the sediment transport rate over the top of the unit bar results in a balance between deposition and erosion of the bar top such that all sediment

transported over the bar top is only deposited at the bar lee if it is deposited at all. Some unit bars will be less tall than the associated dunes and, in this case, they become very difficult to differentiate and may appear as dune fields. Commonly unit bars may have greater amplitude than the associated dunes and they can be much larger. An added complication is that individual unit bars may persist through a number of different magnitude discharge events, whereas dunes may be washed out and reform. Unit bars are ubiquitous and will cause the development of relatively thick compound cross-stratified sets, containing numerous smaller cross bed sets formed by superimposed bedforms. Locally in these large unit bars large set thickness will develop as lee faces amalgamate.

The major changes to complex bars in the very biggest events will result in a lot of these bar deposits being formed in the biggest events and thus in the preserved deposits it is likely that the lower parts of bar complexes will preserve evidence of bigger bedforms – not as a result of being deeper in the channel but because of their formation in the biggest flood events. Only near-surface deposits will be reworked somewhat by the smaller magnitude events. This is consistent with ground-penetrating radar data that show largest and thickest cross-bed sets and scours at and near the base of sections in both the Inkerman site (Fielding *et al.*, 2005b) and at a site upstream near Charters Towers (Fielding *et al.*, 1999).

Antidunes and associated sedimentary structures may be a relatively good indicator of conditions. Antidunes formed in sand or fine gravel, unlike dunes, rapidly establish size related to the flow conditions, thus the wavelength of the bedforms, or possibly the size of the resulting lenses (Froud *et al.*, 2017) may be a better indicator of flow depth and velocity. The problem with this, however, is that the preserved forms are likely to relate to the falling stage conditions rather than peak flow conditions because they easily rework. In addition, they are more likely to be preserved in the deposits from events with rapidly falling stage.

The mean flow velocity can be estimated from the antidune wavelengths using Kennedy's (1961) empirical equation $\lambda = 2\pi V^2/g$, where g is the acceleration due to gravity, V is the mean velocity and λ is antidune wave length. In 2017 at the Inkerman antidune site (Fig. 1C) when antidunes formed with wavelengths of 16.4-28.8 m velocities at the sites when they formed are estimated as 5.1-6.7 m s⁻¹. Given these estimates, using $Fr = V/\sqrt{gd}$ and assuming antidunes formed at Froude Number between 1 and 0.84, suggests water depths when they formed were 2.6-4.6 m. Wavelength of antidunes at the Jarvis field site in 2017 were as much as 30.7 m, implying velocity of 6.9 m s⁻¹ in 4.9 m depth of flow.

Froude *et al.* (2017) used flume observations by Alexander *et al.* (2001) to develop the idea that in flood deposits, gravel lens length parallel to flow may be used to estimate flow velocity. They suggested that mean lens size in one bed may be related to the mean wavelength (temporal and spatial averaging) of the flow that deposited the lenses. If this worked, it would be useful for estimating conditions from deposits when the surface morphology of antidunes is not preserved. Alexander *et al.* (2001) found for sand lenses formed from antidunes in a flume, the ratio of mean lens length to measured water-surface wavelength in the flume was between 0.38 and 0.56. Froude *et al.* (2017) applied this with moderate success to estimate flow velocity in a lahar from gravel lenses in its deposit. In the Burdekin River however, at the Inkerman antidune site the gravel lenses formed by the gravel patches at antidune crests are 0.23 to 0.34 of the mean antidune wavelength within antidune trains. If preserved in the deposits the lenses might be identified by their steep gravel fabric and associated facies, but because of the undersupply of gravel the lens size would underestimate velocities and water depths using Froude *et al.*'s (2017) method unless it becomes possible to estimate the gravel lens to wavelength ratio from the architecture of the deposits. We postulate that this might be achieved in an approximate way using the gravel percent in the deposit.

Vegetation obstacle marks and vegetation-generated bars are commonly observed in the Burdekin River and other rivers of this type (Nakayama *et al.*, 2002). Preserved in situ vegetation

and related sedimentary structures recorded in the deposits are considered characteristic of tropical highly variable channel deposits (Fielding *et al.*, 2009; 2011). They are observed resulting from all flood types but their abundance and character may vary. This is because scour around obstacles (cf. tree trunks or grass clumps) takes time to develop. It is not true to say that the longer flow conditions are maintained the more scour will develop, as the scour depends on the mobility of the bed sediment and the geometry of the obstacle. That said, the shortest flood events may not reach the maximum depths of scour, such that more vegetation will persist on the bed. Vegetation survival is also influenced by duration of submergence, although it is not known how long submergence of different species in this setting will result in plant mortality.

How did five years of antecedent channel-bed plant growth impact the sedimentary response? Before the arrival of TC Debbie in 2017, the river bed downstream of Inkerman Bridge was well covered by tree saplings and other vegetation (Fig. 5A). The runoff in 2017 removed > 50% of this vegetation and cut erosional swales through the sapling groves, 2-3 m deep and gravel-covered (Fig. 5B). Sediment aggradation occurred around surviving vegetation, producing abundant vegetation obstacle marks and tree-triggered linear bars in a manner previously documented at other sites by Fielding *et al.* (1997) and Nakayama *et al.*, 2002).

Conclusions

In the Burdekin River and other similar rivers with very high discharge variability, most sediment movement and morphological change is restricted to a few days each year, while at other times little sediment is moved. The channel deposits are dominated by large-event event deposits with prolonged periods of low flow conditions contributing little sediment volume in comparison. This contrasts with many less variable rivers where channel deposits accumulate more continuously. With the greater inter-annual variability comes greater variability in hydrograph shape, because of

factors such as vegetation density and soil exposure in prolonged arid periods. This also contributes to the more heterogeneous nature of the preserved alluvial record.

In the lower Burdekin River, over the last 50 years, there have been 22 discharge peaks greater $10\,000\text{ m}^3\text{ s}^{-1}$. Analysis of these led to the categorisation of these into three event types, dependent mostly on the rate at which the stage fell. (Type A) The biggest events (arbitrarily classed $>14\,000\text{ m}^3\text{ s}^{-1}$). Eight of these were recorded. In two years, two such peaks were recorded, thus big events happened in six years. (Type B) Events that peak in the $10\,000\text{--}14\,000\text{ m}^3\text{ s}^{-1}$ range with gradual decline. These result from rainfall over the northern catchments, or widespread rainfall, and produce hydrographs with more slowly falling limbs and greater total discharge volume. (Type C) Events that peak in the $10\,000\text{--}14\,000\text{ m}^3\text{ s}^{-1}$ range, with short duration and rapid fall. These result from short-duration rainfall over the eastern sub-catchments, producing an extremely flashy hydrograph.

Rate of change is important, both rise and fall: rise to generate bed waves (possibly triggering unit bars) and fall for preservation of bed features. If peak sediment transport rate lags peak discharge, as in 2000, it is likely that most of the modification of and formation of new unit bars occurs during the falling stage. Consequently in big events with rapid stage fall, little modification of bars occurs. Floods with similar peak discharge magnitude but different rate of decline generate and preserve event deposits and architectures that are different.

Field observations (1998-2017), aerial photographs (1994 – 1998) and satellite images (2006-2017) show that (A) The biggest events ($>14\,000\text{ m}^3\text{ s}^{-1}$) rework large amounts of river bed (cf. Fielding *et al.*, 1999), creating new bars. (B) Events in the $10\,000\text{--}14\,000\text{ m}^3\text{ s}^{-1}$ range with gradual stage decline also change bar position and produce new attached bars. In both A and B, bar surfaces are dominantly sand and gravel sheets. (C) Events that peak in the $10\,000\text{--}14\,000\text{ m}^3\text{ s}^{-1}$ range with short duration and rapid fall rework bar surfaces and produce minor bar accretion. “Washed-out” dunes dominate bar surfaces, and antidunes are preserved. In comparison, antidunes

are not preserved after relatively more slowly waning floods of Type B (i.e. discharge fall over >7 days rather than 2 days). The differences between Type B and C event deposits highlight that: (a) The maximum discharge magnitude does not correlate with the amount of morphological change in the channel and (b) the duration of large discharge events is an important control on the amount of change in morphology of the river bed.

At the study site, velocities and bed conditions in big floods are such to transport boulder grade particles, but these are rarely available at the site. Grade therefore is a very poor indicator of peak flow conditions even in relatively small floods. Due to the co-occurrence of dunes and unit bars, rapid changes in flow depth during an event (such that bedforms do not reach equilibrium with flow conditions), and varying depths of re-working in different event types, cross-bed set thickness is not a good indicator of palaeoflow conditions in these highly variable discharge systems.

Antidunes often form on the river bed and these may have gravel sheets or patches along their crests. Antidunes are easy to identify where gravel crests occur and less obvious on the dry bed when gravel is less abundant. In environments where gravel is less abundant, if antidunes are preserved in the rock record they will be less obvious and diagnostic features for recognizing them in the deposits are poor. In this gravel poor setting the application of the Froude *et al.* (2017) method for estimating antidune wavelength from gravel lens flow-parallel length will tend to underestimate flow velocity and water depth.

The nature of the sedimentary record, in rivers such as the Burdekin, is a complex mosaic biased towards events of relatively large magnitude that gradually decline to base flow. Unlike in less variable systems, channel deposit size is unlikely to be indicative of a channel forming discharge. The size of contained cross-bed sets may give a poor indication of palaeoflow conditions, structures formed by antidunes might be common but difficult to recognize, and more generally, the deposits will not often record peak flood conditions. The relative volume of component event deposits may relate more to flood duration than to magnitude.

Acknowledgements

JA and CH thank University of East Anglia for support of fieldwork costs. CRF fieldwork was supported by the Coffman Endowment in Sedimentary Geology at UNL.

References

- Alexander, J. & Cooker, M. 2016. Moving boulders in flash floods and estimating flow conditions using boulders in ancient deposits. *Sedimentology*, DOI: 10.1111/sed.12274
- Alexander, J. & Fielding, C.R., 1997. Gravel antidunes in the tropical Burdekin Rivers, Queensland, Australia. *Sedimentology*, **44**, 327-337.
- Alexander, J. & Fielding, C.R. 2006. Coarse-grained floodplain deposits in the seasonal tropics: towards a better facies model, *Journal of Sedimentary Research*. 76, 539 – 556.
- Alexander, J., Fielding, C.R. & Pocock, G. D., 1999. Flood behaviour of the Burdekin River, Tropical North Queensland, Australia, *In: Geol. Soc. Lond., Spec. Publ.* 163, 27-40.
- Amos, K.J., Alexander, J., Horn, A., Pocock, G.D. & Fielding, C.R. 2004. Supply limited sediment transport in a high-discharge event of the tropical Burdekin River, North Queensland, Australia. *Sedimentology* 51, 145-162.
- Bainbridge, Z.T., Wolanski, E., Álvarez-Romero, J.G., Lewis, S.E., Brodie, J.E. 2012. Fine sediment and nutrient dynamics related to particle size and floc formation in a Burdekin River flood plume, Australia. *Marine Pollution Bull.* 65, 236-248.
- Bainbridge, Z., Lewis, S., Smithers, S., Wilkinson, S., Douglas, G., Hillier, S., Brodie, J. 2016. Clay mineral source tracing and characterisation of Burdekin River (NE Australia) and flood plume fine sediment. *Jl of Soils & Sedim.* 16, 687-706.

- Bainbridge, Z., Lewis, S., Bartley, R., Fabricius, K., Collier, C., Waterhouse, J., Garzon-Garcia, A., Robson, B., Burton, J., Wenger, A. and J. Brodie. 2018. Fine sediment and particulate organic matter: A review and case study on ridge-to-reef transport, transformations, fates, and impacts on marine ecosystems. *Marine Pollution Bulletin*, 135, 1205-1220.
- Barclay, J., Alexander, J. & Sušnik, J., 2007. Rainfall induced lahars on Montserrat. *Journal of the Geological Society of London* 164, 815-227.
- Bradley, R.W. & Venditti, J.G., 2017. Reevaluating dune scaling relations. *Earth Science Reviews*, 165, 356-376.
- Bridge, J.S., Alexander, J, Collier, R.E.Ll., Gawthorpe, R.L. & Jarvis, J., 1995. Ground-penetrating radar and coring used to study the large-scale structure of point-bar deposits in 3 dimensions. *Sedimentology*, **42**, 839-852.
- Bridge, J.S., Collier, R., Ll. & Alexander, J., 1998. Large-scale structure of Calamus River deposits (braid bars, point bars, and channel fills) revealed using ground-penetrating radar. *Sedimentology*, **45**, 977-986.
- Carling P. 1988. The concept of dominant discharge applied to two gravel-bed streams in relation to channel stability thresholds. *Earth Surface Processes and Landforms*. 13, 355-367.
- Dott, R.H., Jr., 1983. Episodic sedimentation – how normal is average? How rare is rare? Does it matter? *Journal of Sedimentary Petrology*, 53, 5-23.
- Dzulynski and Walton, 1965.
- Fielding, C.R., Alexander, J. & Newman-Sutherland, E., 1997. Preservation of *in situ* vegetation in fluvial channel deposits - data from the modern Burdekin River of North Queensland, Australia. Submitted to *Palaeogeography, Palaeoclimatology, Palaeoecology* **135**, 123-144.

- Fielding, C.R., Alexander, J. & McDonald, R., 1999. Sedimentary facies from GPR surveys of the modern, upper Burdekin River of north Queensland, Australia: consequences of extreme discharge fluctuations. In: Smith, N.D. & Rogers, J. (Eds.), *Current Research in Fluvial Sedimentology*, International Association of Sedimentologists Special Publication, **28**, 347-362.
- Fielding, C.R., Trueman, J. and Alexander J. 2005a. Sharp-based, flood-dominated mouth bar sands from the Burdekin River Delta of northeastern Australia: extending the spectrum of mouth bar facies, geometry and stacking patterns. *Journal of Sedimentary Research*. **75**, 55-66.
- Fielding, C.R., Trueman, J.D. and Alexander, J., 2005b. Sedimentology of the Modern and Holocene Burdekin River Delta of North Queensland, Australia – controlled by river output, not by waves and tides: Giosan, L. and Bhattacharya, J., eds., *Deltas, New and Old*: SEPM Special publication, **83**, 467-496.
- Fielding, C.R., Allen, J.P., Alexander J. & Gibling, M.R. 2009. Facies model for fluvial systems in the seasonal tropics and subtropics. *Geology*, *37* (7), 623-626. DOI: 10.1130/G25727A.1
- Fielding, C.R., Allen, J.P., Alexander, J., Gibling, M.R., Rygel, M.C. and Calder, J.H. 2011. Fluvial systems and their deposits in hot, seasonal semiarid and subhumid settings: modern and ancient examples, *In*: SEPM spec. publ. 97, 89-111. ISBN 978-1-56576-305-0.
- Fielding, C. R., Alexander, J. & Allen, J. P. 2018. The role of discharge variability in the formation and preservation of alluvial sediment bodies. *Sedimentary Geology* 365, p. 1-20.
- Froude, M.J., Alexander, J., Barclay, J & Cole, P. 2017. Interpreting flash flood palaeoflow parameters from antidunes and gravel lenses: An example from Montserrat, West Indies. *Sedimentology*, Volume 64, 1817–1845. DOI: 10.1111/sed.12375
- Groisman, P.Ya., Knight, R.W., Easterling, D.R., Karl, T.R., Hegerl, G.C. and Razuvaev, V.N. 2005. Trends in intense precipitation in the climate record. *Journal of Climate* 18, 1326-1350.

Herbert, C.M., & Alexander, J. 2018. Bottomset architecture formed in the troughs of dunes and unit bars. *Journal of Sedimentary Research* 88, 1–32.

Herbert, C., Alexander, J., Amos, K.J. and Fielding C.R. *submitted* Unit bar architecture in a highly unsteady fluvial regime: examples from the Burdekin River, Australia. *Sedimentology*.

Horn, J.D., Fielding, C.R., Joeckel, R.M., 2012a. Revision of Platte River alluvial facies model through observations of extant channels and barforms, and subsurface alluvial valley fills. *Journal of Sedimentary Research* 82, 72-91.

Joeckel, R.M., Henebry, G.M., 2008. Channel and island change in the lower Platte River, Eastern Nebraska, USA: 1855-2005. *Geomorphology* 102, 407-418.

Lewis, S.E., Bainbridge, Z.T, Kuhnert, P.M., Sherman, B.S., Henderson, B., Dougall, C., Cooper, M. and J.E. Brodie. 2013. Calculating sediment trapping efficiencies for reservoirs in tropical settings: A case study from the Burdekin Falls Dam, NE Australia. *Water Resources Research* 49, 1017–1029, doi:10.1002/wrcr.20117.

Maher, B.A., Watkins, S.J., Fielding, C.R., Alexander, J. & Brunskill, G. 2009. Sediment sourcing by magnetic ‘fingerprinting’ of transportable sand fractions in a tropical fluvial, estuarine and marine context. *Sedimentology* 56, 841-861.

Nakayama, K. Fielding, C.R. & Alexander, J. 2002. Variation in character and preservation potential of vegetation-induced obstacle marks in the variable discharge Burdekin River of north Queensland, Australia. *Sedimentary Geology*, 149, 199-218.

Neil, D.T., Orpin, A.R., Ridd, P.V., Yu, B. (2002) Sediment yield and impacts from river catchments to the Great Barrier Reef lagoon *Australian Journal of Marine and Freshwater Research* 53, 733-752.

Prosser, I.P., Moran, C.J., Lu, H., Scott, A., Rustomji, P., Stevenson, J., Priestly, G., Roth, C.H., Post, D. (2002) Regional patterns of erosion and sediment transport in the Burdekin River catchment CSIRO Land and Water, Technical Report 5/02, 44.

Rose, C.W., Shellberg, J.G., Brooks, A.P. 2015. Modelling suspended sediment concentration and load in a transport-limited alluvial gully in northern Queensland, Australia. *Earth Surface Processes and Landforms* 40, 1291-1303.

Sadler, P.M., 1983. Is the present long enough to measure the past? *Nature*, 302, p.752.

Sambrook Smith, G.H., Best, J.L., Ashworth, P.J., Lane, S.N., Parker, N.O., Lunt, I.A., Thomas, R.E., Simpson, C.J., 2010. Can we distinguish flood frequency and magnitude in the sedimentological record of rivers? *Geology*, 38, 579-582.

Smith, N.D. 1974. Sedimentology and bar formation in the upper Kicking Horse River: a braided outwash stream. *Journal of Geology* 82, 205-223.

Williams, G.P. 1978. Bank-full discharge of rivers, *Water Resources Research*, 14, 1141-1154.

Figures

Figure 1. **A.** Catchment map showing the location of the study site. Gauging stations are S Sellhiem, C Clare, U Urannah, Rain gauges K Kalamia Estate, M Majors Creek. **B.** Location map of area of Clare to coast. ab represents Airlie Beach, **C.** Satellite image of the study reach during the 2017 dry season (image dated 19/08/2017, obtained from: Google Earth, 2019 CNES/Airbus). The area beyond the channel margins has been faded. Black lines labelled A, B and C show positions of elevation transects presented in Fig. 4. Ellipses labelled I and J identify the antidune sites referred to in the text as Inkerman and Jarvisfield.

Figure 2. **A.** Time series of discharge recorded at Clare showing the magnitude of peak events and the variation within and between years. The discharge in the Burdekin River has been monitored at Clare (52 km from the river mouth, drainage basin above Clare is 129 876 km²) continuously since 1949. Burdekin Falls Dam, 108 km upstream of Clare was completed in 1987. **B.** hydrographs for 1997 discharge at Sellhiem and Clare gauging stations. Data source; Australian Government, Bureau of Meteorology, <http://www.bom.gov.au/metadata/catalogue/view/ANZCW0503900339.shtml>.

Figure 3. Catchment maps: **A.** The tracks of the eye of tropical cyclone that were associated with large rain rainfall events. The rainfall covers a large area around the line of the track. **B.** Illustrating the main sub-catchments and the mean rainfall pattern (data from www.bom.gov.au/climate/data/index.shtml), **C.** land use after State of Queensland 2018 land use map, **D.** Simplified geological map based on Prosser *et al.* (2002).

Figure 4. Elevation data for the 2017 study site at channel cross-sections A, B and C; the locations of these presented in Fig. 1C. Complete cross-sections obtained from LiDAR data, collected in the 2009 dry season (between 10th June – 10th September; Queensland Government Department of Natural Resources, Mines and Energy): 1m grid size, vertical accuracy ± 10 cm (1 σ), horizontal accuracy ± 20 cm (1 σ). Real Time Kinematic GPS survey data (horizontal accuracy ± 1 cm, vertical accuracy ± 2 cm) were collected 25th – 28th July 2017.

Figure 5. Photographs from Inkerman Bridge before and after the 2017 event. **A.** before photograph, taken on 15th July 2016. **B.** after, photographed 22 July 2017. Not in the remains of old bridge supports visible in both pictures.

Figure 6. Burdekin Catchment maps of rain fall for 7 days: **A.** before a peak of a big discharge event and, **B.** seven days post peak discharge of events discusses in this paper. The seven-day rainfall maps are based on those generated at <http://www.bom.gov.au/jsp/awap/rain/archive.jsp> .

Figure 7. Hydrographs for some of the event discussed in this paper. **A.** Hydrographs for the 30 days starting from the peak of the discharge recorded at Clare. The distinction between Type 1 and 2 discharge events is see in the rate of decline of the flood and the flood duration. **B.** The discharge recorded at Clare from 1st January to 1st April 1991 to show multiple peaks. The discharge data is from Australian Government, Bureau of Meteorology. Data source; <http://www.bom.gov.au/metadata/catalogue/view/ANZCW0503900339.shtml>.

Figure 8. Photographs of facies and features: **A.** Cobbles lodged in *Melaleuca argentea* sapling c. 0.5 m above bed in the 2017 event, **B.** Extensive *sand sheets* occur both as components of unit bars and adjacent to unit bars at all elevations in the channel. This view taken in July 2017 is looking upstream towards the Inkerman bridge. Notice the tire tracks across the sand from bottom right, giving a sense of scale. **C.** Mud drape over small dunes in July 2017. The spade is 0.60 m long. **D.** Where the mud drapes are millimetres thick and resting on coarse sand, desiccation can lead to mud

curl formation. In this photograph taken in 2017 the mud was deposited in the lee of a unit bar near the low flow channel. The car tracks indicate the scale. **E.** Looking down on a gravel sheet in 2017. The spade is 0.60 m long, **F.** Gravel sheet 2017. The blue line is about 0.5 m long.

Figure 9. Photographs of bedforms and features: **A.** antidunes appear as an elongate gravel patch. The person in the background is 1.80 m tall. **B.** antidunes shown in plan and cross section. The deposits consist of a lens of sandy gravel. The yellow notebook is 0.20 m long. **C.** unit bar, the spade is 0.60 m long. **D.** section through unit bar, the spade is 0.60 m long. **E.** Vegetation obstacle marks, the rucksack is 0.50 m tall. **F** Vegetation-generated bar formed around in situ trees. The bar was about 1.5 m high, tens of metres long in a of mature *Melaleuca argentea* trees near the low water channel of the Bowen River upstream of the Mt Wyatt crossing. This bar was covered by surface carapace of pebble to cobble gravel. The cutface in the photograph revealed much of this bar is made up of medium-grained sand, with minor very fine- and fine-grained sand lenses, gravely sand lens, and minor mud partings. Sand beds are arranged in a complex cross-cutting pattern indicating multi-directional cross-bedding as the dominant internal structure. The red notebook on top of the bar is 0.20 m long

Tables

Table 1. Weather conditions and peak discharge of flow events with peak magnitude greater than 10 000 m³ s⁻¹ since 1977. The largest class of events' peak discharges are highlighted in bold.

Discharge data from Australian Government Bureau of Meteorology.

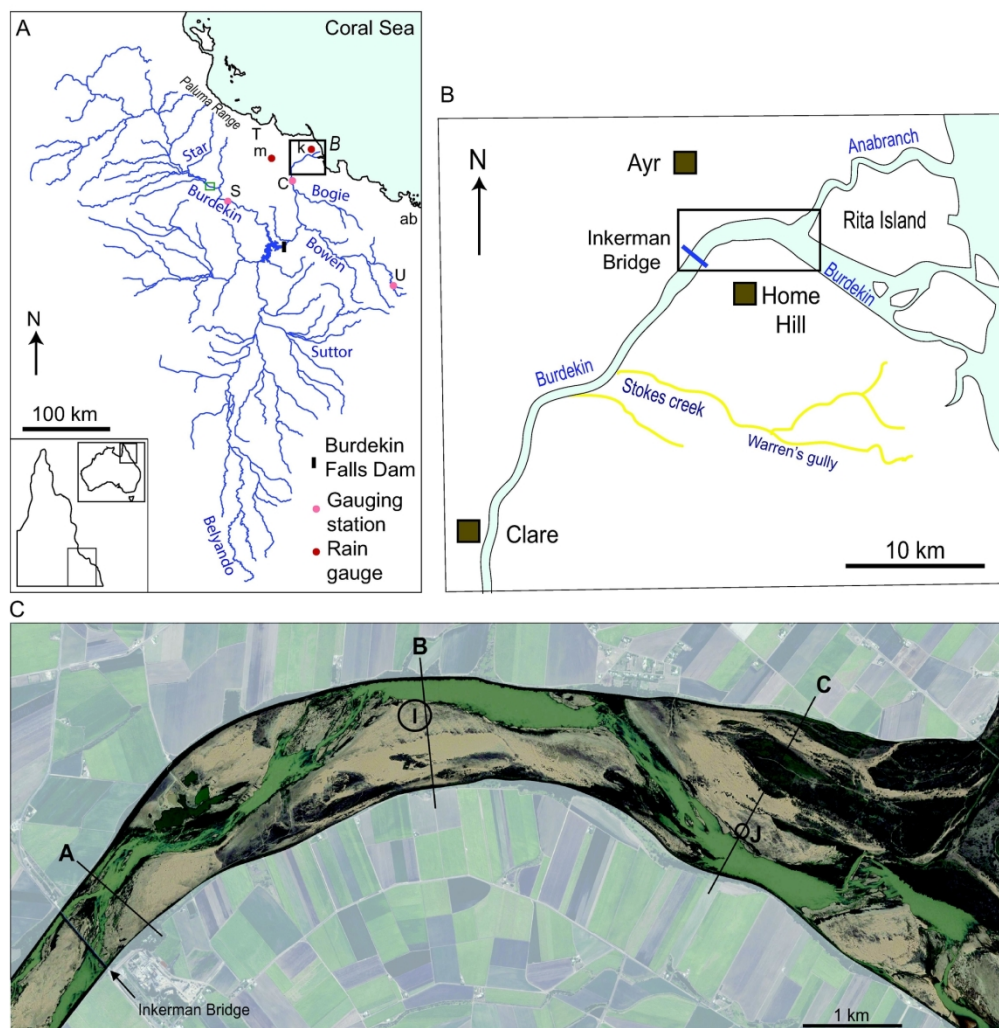


Figure 1. A. Catchment map showing the location of the study site. Gauging stations are S Sellhiem, C Clare, U Urannah, Rain gauges K Kalamia Estate, M Majors Creek. B. Location map of area of Clare to coast. ab represents Airlie Beach, C. Satellite image of the study reach during the 2017 dry season (image dated 19/08/2017, obtained from: Google Earth, 2019 CNES/Airbus). The area beyond the channel margins has been faded. Black lines labelled A, B and C show positions of elevation transects presented in Fig. 4. Ellipses labelled I and J identify the antidune sites referred to in the text as Inkerman and Jarvisfield.

174x188mm (300 x 300 DPI)

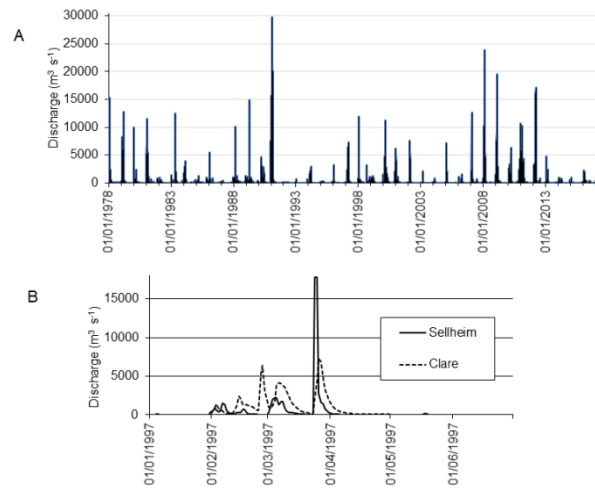


Figure 2. A. Time series of discharge recorded at Clare showing the magnitude of peak events and the variation within and between years. The discharge in the Burdekin River has been monitored at Clare (52 km from the river mouth, drainage basin above Clare is 129 876 km²) continuously since 1949. Burdekin Falls Dam, 108 km upstream of Clare was completed in 1987. B. hydrographs for 1997 discharge at Selhiem and Clare gauging stations. Data source; Australian Government, Bureau of Meteorology, <http://www.bom.gov.au/metadata/catalogue/view/ANZCW0503900339.shtml>.

338x190mm (96 x 96 DPI)

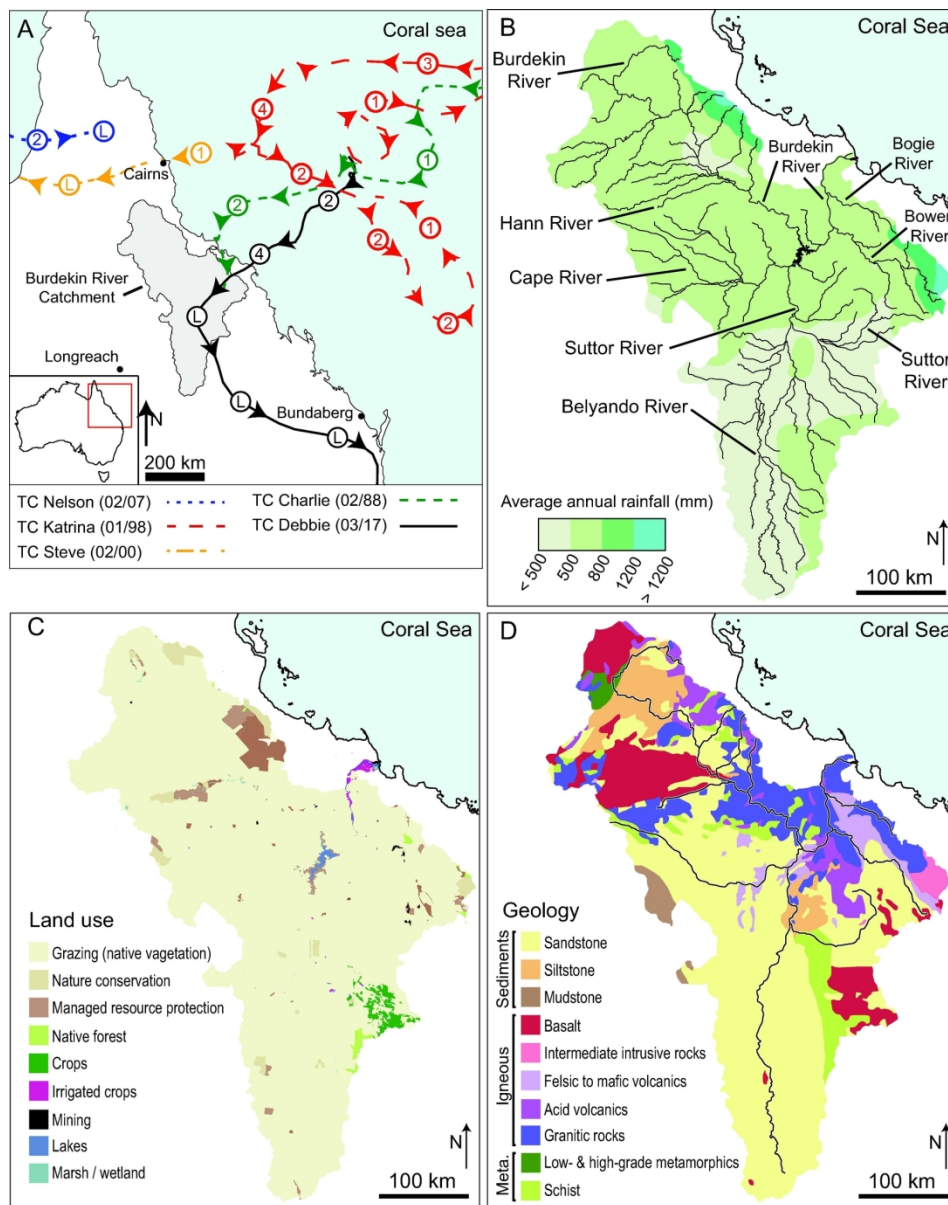


Figure 3. Catchment maps: A. The tracks of the eye of tropical cyclone that were associated with large rain rainfall events. The rainfall covers a large area around the line of the track. B. Illustrating the main sub-catchments and the mean rainfall pattern (data from www.bom.gov.au/climate/data/index.shtml), C. land use after State of Queensland 2018 land use map, D. Simplified geological map based on Prosser et al. (2002).

161x204mm (300 x 300 DPI)

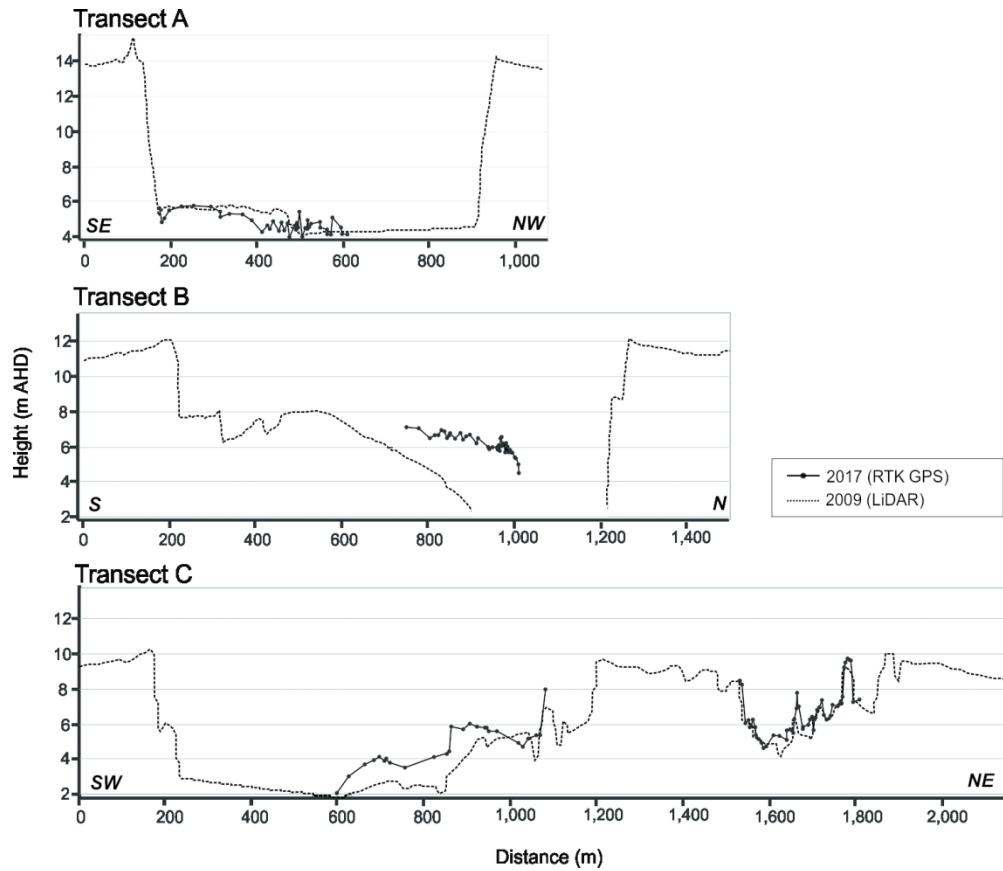


Figure 4. Elevation data for the 2017 study site at channel cross-sections A, B and C; the locations of these presented in Fig. 1C. Complete cross-sections obtained from LiDAR data, collected in the 2009 dry season (between 10th June – 10th September; Queensland Government Department of Natural Resources, Mines and Energy): 1m grid size, vertical accuracy ± 10 cm (1σ), horizontal accuracy ± 20 cm (1σ). Real Time Kinematic GPS survey data (horizontal accuracy ± 1 cm, vertical accuracy ± 2 cm) were collected 25th – 28th July 2017.

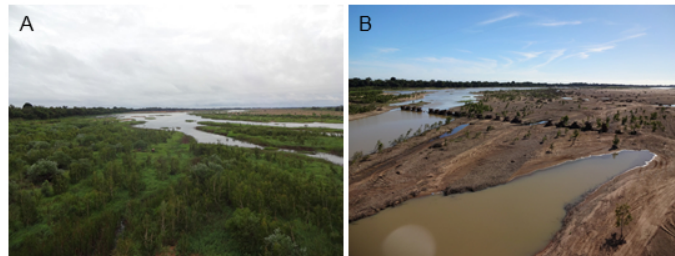


Figure 5. Photographs from Inkerman Bridge before and after the 2017 event. A. before photograph, taken on 15th July 2016. B. after, photographed 22 July 2017. Not in the remains of old bridge supports visible in both pictures.

190x254mm (96 x 96 DPI)

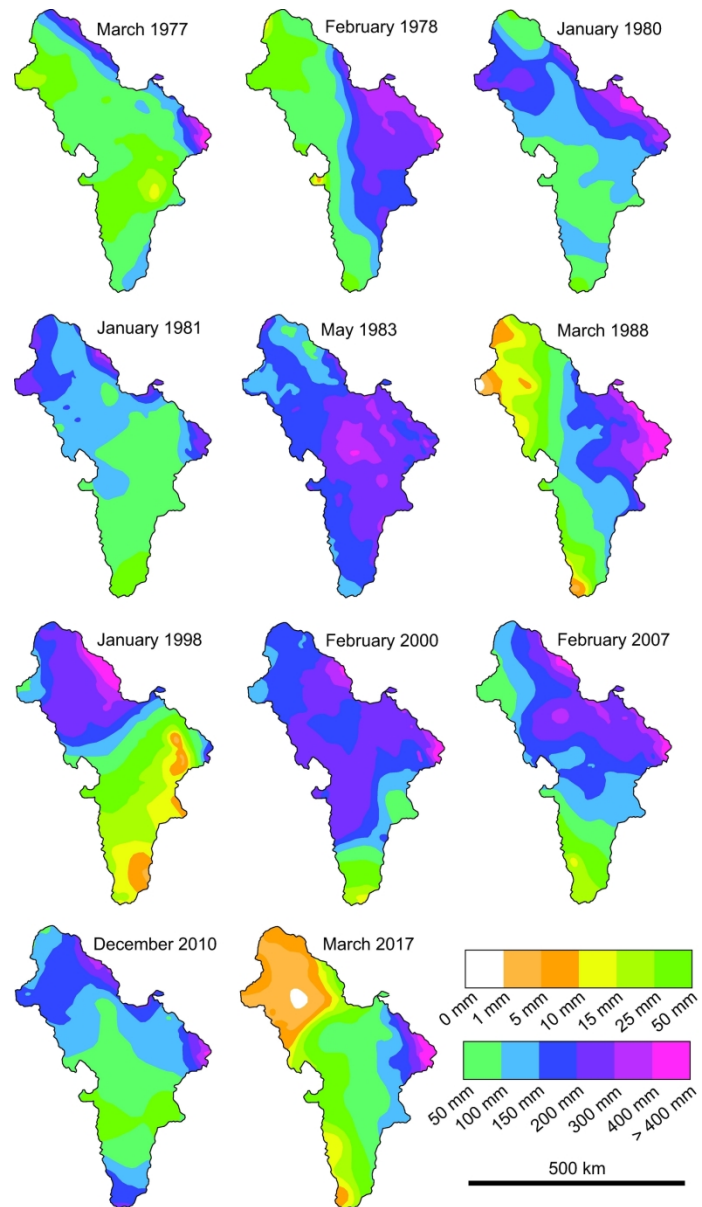


Figure 6.A Burdekin Catchment maps of rain fall for 7 days: A. before a peak of a big discharge event.. The seven-day rainfall maps are based on those generated at <http://www.bom.gov.au/jsp/awap/rain/archive.jsp>

153x267mm (300 x 300 DPI)

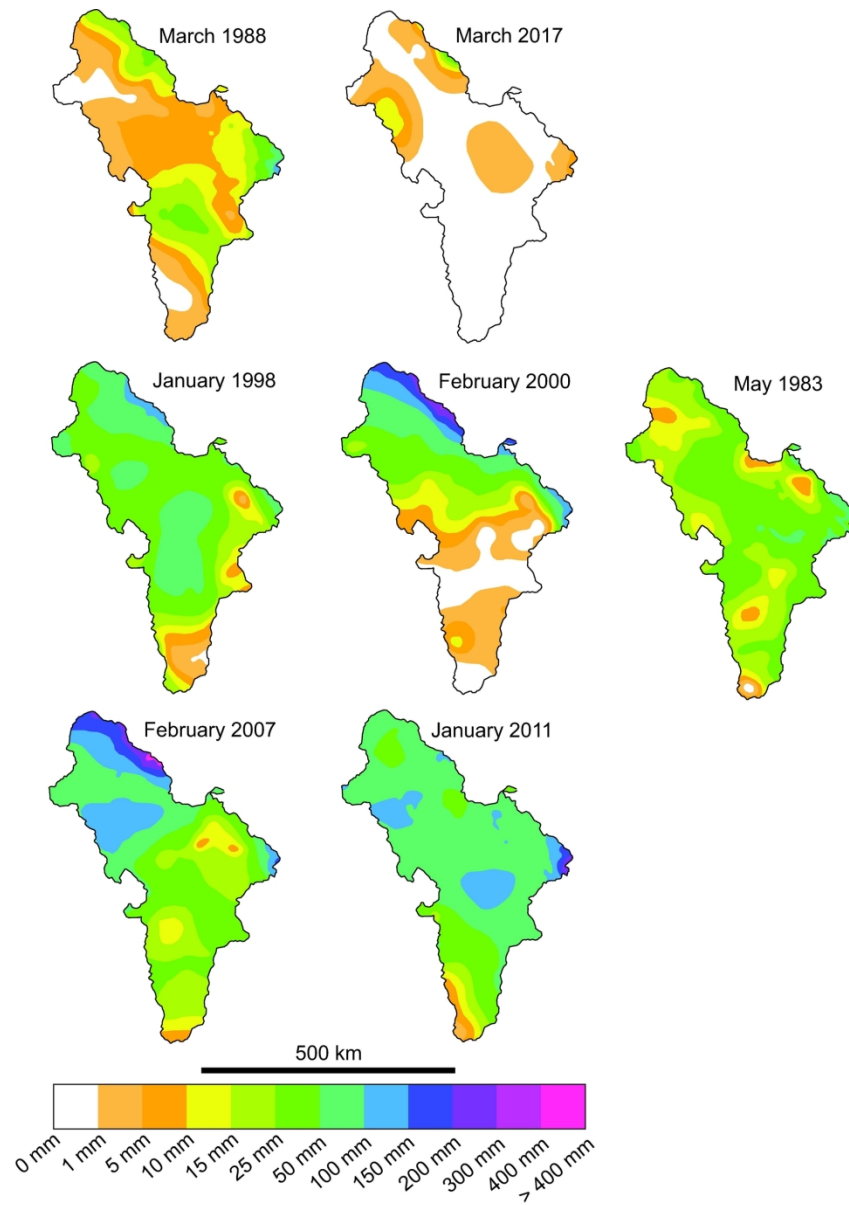


Figure 6 B. seven days post peak discharge of events discusses in this paper. The seven-day rainfall maps are based on those generated at <http://www.bom.gov.au/jsp/awap/rain/archive.jsp> .

160x228mm (300 x 300 DPI)

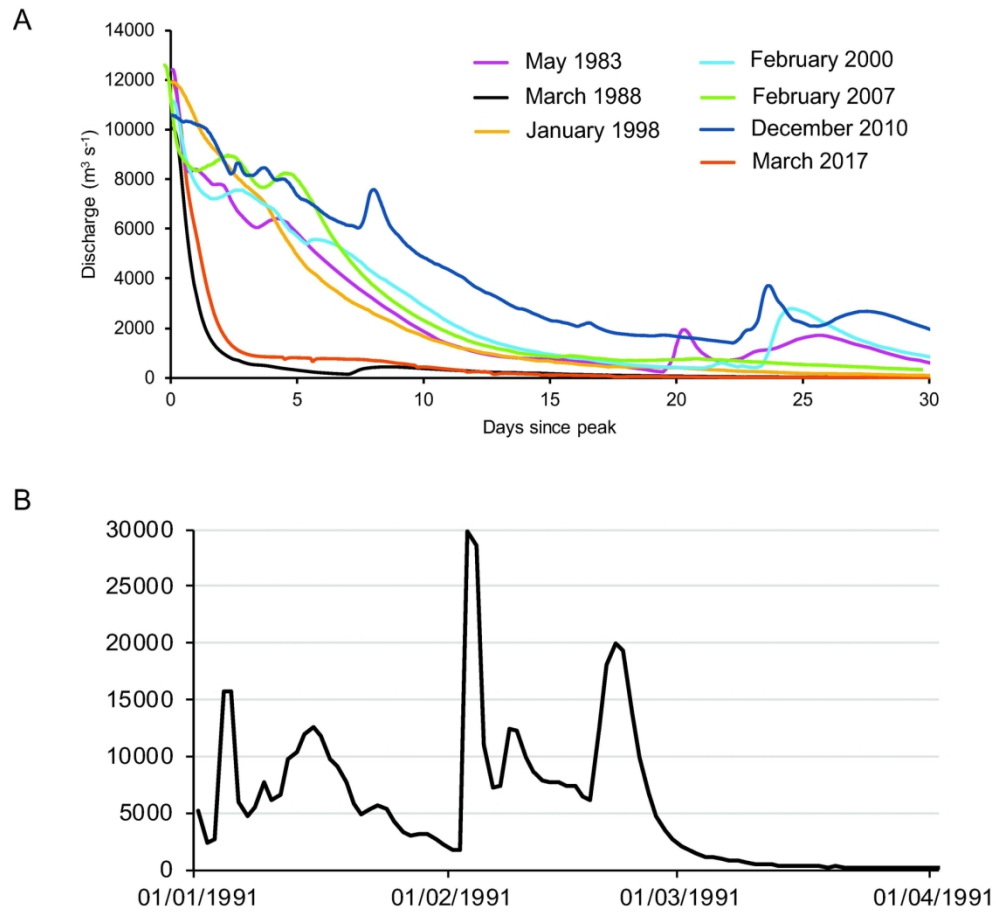


Figure 7. Hydrographs for some of the event discussed in this paper. A. Hydrographs for the 30 days starting from the peak of the discharge recorded at Clare. The distinction between Type 1 and 2 discharge events is see in the rate of decline of the flood and the flood duration. B. The discharge recorded at Clare from 1st January to 1st April 1991 to show multiple peaks. The discharge data is from Australian Government, Bureau of Meteorology. Data source; <http://www.bom.gov.au/metadata/catalogue/view/ANZCW0503900339.shtml>.

159x147mm (300 x 300 DPI)



Figure 8. Photographs of facies and features: A. Cobbles lodged in *Melaleuca argentea* sapling c. 0.5 m above bed in the 2017 event, B. Extensive sand sheets occur both as components of unit bars and adjacent to unit bars at all elevations in the channel. This view taken in July 2017 is looking upstream towards the Inkerman bridge. Notice the tire tracks across the sand from bottom right, giving a sense of scale. C. Mud drape over small dunes in July 2017. The spade is 0.60 m long. D. Where the mud drapes are millimetres thick and resting on coarse sand, desiccation can lead to mud curl formation. In this photograph taken in 2017 the mud was deposited in the lee of a unit bar near the low flow channel. The car tracks indicate the scale. E. Looking down on a gravel sheet in 2017. The spade is 0.60 m long, F. Gravel sheet 2017. The blue line is about 0.5 m long.

190x254mm (96 x 96 DPI)

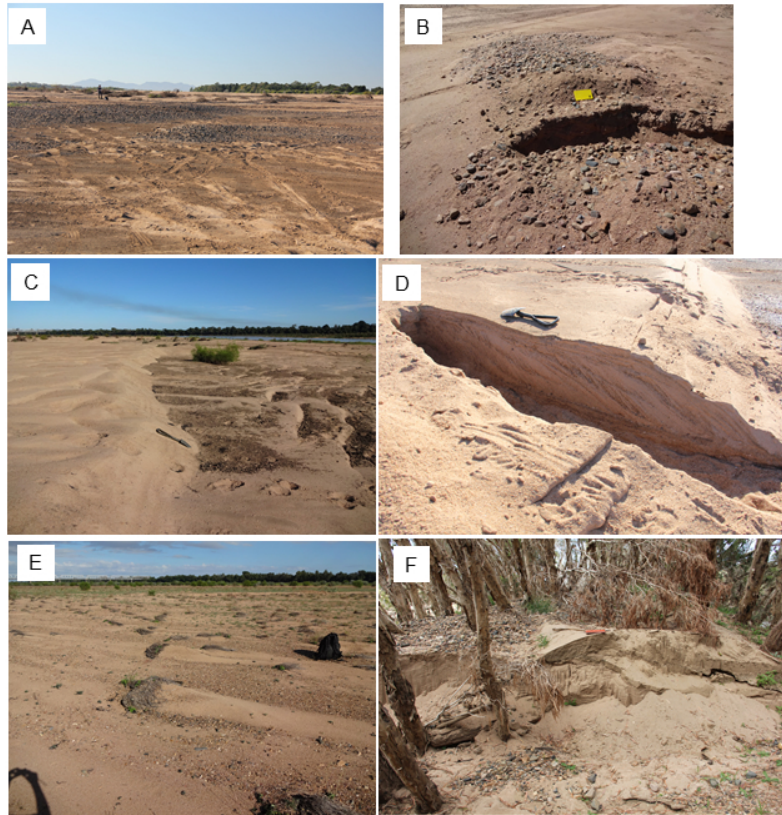


Figure 9. Photographs of bedforms and features: A. antidunes appear as an elongate gravel patch. The person in the background is 1.80 m tall. B. antidunes shown in plan and cross section. The deposits consist of a lens of sandy gravel. The yellow notebook is 0.20 m long. C. unit bar, the spade is 0.60 m long. D. section through unit bar, the spade is 0.60 m long. E. Vegetation obstacle marks, the rucksack is 0.50 m tall. F. Vegetation-generated bar formed around in situ trees. The bar was about 1.5 m high, tens of metres long in a row of mature *Melaleuca argentea* trees near the low water channel of the Bowen River upstream of the Mt Wyatt crossing. This bar was covered by surface carapace of pebble to cobble gravel. The cutface in the photograph revealed much of this bar is made up of medium-grained sand, with minor very fine- and fine-grained sand lenses, gravelly sand lens, and minor mud partings. Sand beds are arranged in a complex cross-cutting pattern indicating multi-directional cross-bedding as the dominant internal structure. The red notebook on top of the bar is 0.20 m long.

190x254mm (96 x 96 DPI)

Table 1. Weather conditions and peak discharge of big flow events in the Burdekin River since 1977. Peak discharge of the largest class of events ($>14\,000\text{ m}^3\text{ s}^{-1}$) are highlighted in bold. Discharge data from Australian Government Bureau of Meteorology.

Year month	Peak discharge at Clare ($\text{m}^3\text{ s}^{-1}$)	Contributing weather	Contributing areas
1978 February	15266	TC Gwen, that started in the Gulf of Carpentaria and tracked southeast across Cape York.	Rain over the entire catchment, heaviest in the east.
1979 March	12795	TC Kerry over the Corral Sea moved up and down along the coast.	Intense rainfall particularly in East of the catchment.
1981 January	11527	Monsoon development. No TC	Rain over the entire catchment, heaviest in the north and on the eastern fringes.
1983 May	12415	Monsoon development. No TC	Heavy rain over the entire catchment, heaviest in centre and east.
1988 March	10029	TC Charlie tracked southwest from the Coral Sea, making landfall southeast of Townsville (Fig. 1A). Once making landfall, it travelled ca. 150 km inland over the eastern parts of the catchment, before dying out.	Rain mostly in the centre and east of the catchment, heaviest in the east.
1989 April	14924	TC Aivu made landfall near the mouth of the Burdekin River on 4 th April and moved west across the catchment.	Heavy rain along east of the catchment moved west across the catchment.
1991 January	15709	Well-developed monsoon, with addition of a tropical low over the Bowen subcatchment.	Widespread rain in January-February, with added intense rain over Bowen subcatchment in February associated with tropical low.
February	12632		
	29825 12269 20002		
1998 January	11905	Low pressure light rain followed by monsoon trough and then three TCs in the Coral Sea (e.g. TC Katrina; Fig. 3) produced rain on coast.	Rain mostly in the north and centre of the catchment, heaviest in the north.
2000 February	11155	TC Steve's centre tracked north of catchment (Fig. 3). This was followed by the monsoon trough moving north. up the coast and	Rain mostly in north of catchment from TC Steve. Monsoon trough rain was widespread and heavier along

2007 February	12590	inland. Monsoon trough. TC Nelson (Fig. 3) may have caused some of the rainfall after the peak event.	the coast. Rain over the entire catchment, heaviest in the east and north.
2008 January February February	10215 23908 15005	Ex-TC Helen tracked south in January and then a monsoon trough developed in February.	Widespread rain produced triple-peak hydrograph
2009 February February	19515 15969	Active monsoon trough resulted in the development of TC Ellie. Ellie made landfall north of Townsville and tracked to Gulf of Carpentaria. A trough then formed over the NW Coral Sea	Widespread rain with intense rain in south of the catchment later producing second peak
2010 December	10585	Monsoon trough. No TC.	Rain over the entire catchment, heaviest in the north as well as the eastern and southern fringes.
2012 March	17144	A tropical low tracked across the catchment from west to east.	Widespread rain over the catchment
2017 March	11955	TC Debbie made landfall close to the eastern catchment and tracked inland, southwest and then south (Fig. 3). Intense rain was limited to the south and east.	Rain short duration and intense on the east of the catchment, heaviest on the eastern fringes.